Internal dynamics of actin structures involved in the cell motility and adhesion: modeling of the podosomes at the molecular level.

Shiqiong Hu, Thierry Biben, Xianghui Wang, Pierre Jurdic, Jean-Christophe Géminard

Internal dynamics of actin structures involved in the cell motility and adhesion: modeling of the podosomes at the molecular level.

S. Hu[a,c], T. Biben[b], X. Wang[c], P. Jurdic[d], J.-C. Géminard[a,*]

[a] *Laboratoire de Physique, Université de Lyon, Ecole Normale Supérieure de Lyon - CNRS, 69364 Lyon cedex 07, France.*
[b] *Laboratoire de Physique de la Matière Condensée et Nanostructures, Université de Lyon, Université Lyon I - CNRS, 69622 Villeurbanne, France .*
[c] *State Key Laboratory of Precision Spectroscopy, Department of Physics, East China Normal University, Shanghai 200062, China.*
[d] *Institut de Génomique Fonctionnelle de Lyon, Université de Lyon, Ecole Normale Supérieure de Lyon - CNRS, 69364 Lyon cedex 07, France.*

Abstract

Podosomes are involved in the spreading and motility of various cells to a solid substrate. These dynamical structures, which have been proven to consist of a dense actin core surrounded by an actin cloud, nucleate when the cell comes in the vicinity of a substrate. During the cell spreading or motion, the podosomes exhibit collective dynamical behaviors, forming clusters and rings. We design a simple model aiming at the description of internal molecular turnover in a single podosome: actin filaments form a brush which grows from the cellular membrane whereas their size is regulated by the action of a severing agent, the gelsolin. In this framework, the characteristic sizes of the core and of the cloud, as well as the associated characteristic times are expressed in terms of basic ingredients. Moreover, the collocation of the actin and gelsolin in the podosome is understood as a natural result of the internal dynamics.

Keywords: Bone resorption, Osteoclast, Cellular attachment, Molecular turnover

*corresponding author
Email address: jean-christophe.geminard@ens-lyon.fr (J.-C. Géminard)

1. Introduction

All along the adult life, two types of cell insure the permanent renewal of the bone material: the osteoclasts, which resorb the bone, and the osteoblasts, which secrete new material replacing the old one. When an osteoclast encounters a substrate, small structures, the podosomes, appear in the contact region. Podosomes are actin structures involved in the spreading and motility of various cells (dendritic cells, osteoclasts, macrophages) to a solid substrate [1, 2, 3, 4]. They have been proven to consist of a dense actin core surrounded by an actin cloud [5, 6].

In an initial stage, the podosomes form aggregates (*clusters*) in which they remain randomly distributed with a distance of about 1.4 μm between them. In a second stage, podosomes disappear at the center of the initial cluster, forming then an annulus (*ring*) that migrates toward the periphery of the contact region with a velocity of about 2 μm/min. During this process, podosomes which remain immobile, preferably disappear along the inner boundary of the annulus whereas others nucleate at the outer boundary. The whole process results in an increase of the surface area of the contact region between the cell and the substrate [5].

In the confocal microscope, the apparent shape of a podosome is a cone of typical height $h \simeq 0.5$ μm and base radius $r_p \simeq 0.15$ μm. It is made of a dense assembly of actin filaments, the *core*, preferably oriented along the perpendicular to the cell membrane [7]. Interestingly, FRAP (Fluorescence Recovery After Photobleaching) experiments have proven that podosomes are dynamical structures in spite of their stationary shape during their lifespan which is about 2 min [5]: the podosomes grow during about 30 s before they reach an apparent steady-state during which the filaments continuously grow from the cellular membrane.

The mechanisms that regulate these structures are not known at present but probably involve actin regulators that are specifically found in podosomes, like cortactin and Wiskott-Aldrich syndrome protein (WASP), which localize directly underneath the podosome [6]. Among them, the gelsolin, an actin severing agent, has been proven to be essential for the podosome regulation [8, 9]. Fluorescence experiments in which the actin and the gelsolin are marked by different fluorescent dyes show that the activity of the two molecules collocate: the concentration of the gelsolin is large in the podosome core as well as in the surrounding cloud (Fig. 1).

In a first approach [10], we focussed on the dynamics of the actin in the

core and in the cloud. Reducing the complex biological system to a simplified model involving only the synthesis of actin filaments at the cell membrane and the severing, we accounted for the observed apparent shape of the single podosome and for experimental FRAP results, which proved that podosomes are dynamical structures. However, the previous model could not account for the colocalization of the gelsolin and actin fluorescence signals. In the present Letter, introducing equations governing the activity of the gelsolin molecule, we propose a far more complete model which explains why the concentration of the gelsolin is large in both the core and the cloud and we discuss the consequences for the dynamics of the podosomal structures.

2. Model and definitions

Following the same idea as developed in [10], we consider a podosome as a dense assembly of independent actin filaments, the *actin core*. Seeking for simplicity, and in accordance with recent experimental results [11], we will consider that the filaments are not branched. Each filament is supposed to grow, from a nucleation site located at the cell membrane, by addition of monomers whereas its size is limited by the action of the severing molecule, the *gelsolin* (Fig. 2). The filaments that are released from the core diffuse freely in the *cytoplasm* (the intra cellular medium) and form the *actin cloud* [5]. In the cloud, the free filaments are subsequently cut by the gelsolin.

In order to account for the dynamics of the actin in the core, we consider the probability $b_n(t)$, at time t, for a filament attached to the nucleation site to consist of $(n+1)$ monomers, linked by n bonds. The number of filaments in the core is M and the typical radius of the structure at the membrane, σ (Note that no additional assumption about the geometrical arrangement of the filaments in the core is made). For the freely-diffusing filaments, we consider $c_n(\vec{r},t)$ the concentration, at time t and position $\vec{r}$, of the filaments which consist of $(n+1)$ monomers linked by n bonds. In accordance, $c_0(\vec{r},t)$ denotes the concentration of the freely-diffusing actin monomers.

In the core, the growth of the filaments is insured by the addition of actin monomers from a nucleation site with the frequency v. The growth velocity of the filaments is thus av, where a (~ 2.7 nm) denotes the diameter of the actin monomer. Seeking for simplicity, we will assume that the typical size σ of the nucleation site is small compared to the typical diffusion length so that the local concentration of the actin monomer, at time t, is $c_0(\vec{0},t)$, constant

in the podosome core and, thus, that the polymerization frequency v, which might depend on c_0, is the same for all the filaments [12].

The severing of the actin filaments is due to the action of the gelsolin [13]. Gelsolin is a potent actin-filament severing-protein. In the presence of micromolar concentration of calcium, gelsolin rapidly binds to the side of actin filaments, which is followed by a relatively slow severing process. After severing, the gelsolin caps the barbed end. We mention that the activity of the severing agent is also regulated by other species, especially phospholipids (PIP, PIP_2,... [13]).

In order to account for the severing, in the framework of our simplistic model, we shall keep only the basic ingredients of the gelsolin severing activity. We will assume that the concentration of calcium ions is large and that their diffusion is fast. In this limit, the activity of the gelsolin will not be limited by any kinetic effect associated with that of the calcium ions. In the same way, seeking for simplicity, we will neglect any effect associated with the phospholipids. Thus, the gelsolin diffuses in the cytoplasm with the diffusion coefficient D_g and attaches to any available bond between two actin monomers with the kinetic constant k_{on}. Once a bond is occupied by a gelsolin molecule, it is cut after the typical time $\tau \equiv 1/\beta$. Even if the gelsolin molecule has been recognized to cap the barbed end, we will assume that the molecule is released in the cytoplasm right after severing. The main reason for this choice is that the orientation of the actin filaments in the podosome core is not known at present. Thus, considering the internal dynamics of the core, we are unable to decide if the gelsolin molecule remains attached to the filament inside the core or diffuses away with the released part. Both situations can be considered in the model, leading to slightly different systems of equations. However, capping does not change the qualitative behavior of these equations and we shall ignore it in this first approach.

The dynamics of the gelsolin will be accounted for by considering its local concentration in the cytoplasm $g(\vec{r})$ and the probabilities $f_n(t)$, respectively $h_n(\vec{r}, t)$, for one bond between two actin monomers in the core, respectively in the cytoplasm, to be occupied by a gelsolin molecule. In order to make these definitions clear, we consider a first example and write the total number of gelsolin molecules bound to filaments having n bonds in the core. In average, nf_n gelsolin molecules are attached to one filament having n bonds in the core. In addition, the number of filaments having n bonds is Mb_n. As a result, the total number of gelsolin molecules bound to all the filaments having n bonds in the core is $(Mb_n) \times (nf_n) = M(nf_nb_n)$. Second example,

locally in the cloud, at time t and position $\vec{r}$, the total concentration of the gelsolin, free or bound to filaments, is $c_g \equiv g(\vec{r},t) + \sum_{n=1}^{\infty} n h_n(\vec{r},t) c_n(\vec{r},t)$.

The actin monomers and the filaments diffuse in the cytoplasm when not attached to the core. We denote D_0 the diffusion coefficient of the actin monomers. Following Einstein's prescription [14], we can assume that the diffusion coefficient of an actin filament made of $(n+1)$ monomers, free of gelsolin molecule ($h_n = 0$), decreases with its molecular weight according to $D_n = D_0/(n+1)$. When gelsolin molecules are attached to the filament, we can accordingly assume that:

$$D_n \equiv \frac{D_0}{1 + n(1 + \alpha h_n)}, \tag{1}$$

where $\alpha \equiv m_g/m_a \simeq 2.1$ is the ratio of the mass $m_g \simeq 90$ kDa of the gelsolin molecule to the mass $m_a \simeq 43$ kDa of the actin monomer [12].

3. Set of equations governing the dynamics

In the present section, we shall establish the set of equations governing the dynamics of the distribution b_n, diffusion fields, g and c_n, as well as of the probabilities, f_n and h_n, which account for the dynamics of the podosome core and surrounding cloud.

3.1. The core

The internal dynamics of the actin core is accounted for by the distribution $b_n(t)$ of the filament length and the probability f_n which describes the occupation of the bonds by the gelsolin molecule.

Taking into account the polymerization at the nucleation site and the severing, the equation governing the temporal evolution of the distribution $b_n(t)$ is given by:

$$\frac{db_n}{dt} = v(b_{n-1} - b_n) - \beta n f_n b_n + \beta \sum_{k=n+1}^{\infty} f_k b_k. \tag{2}$$

The first term accounts for the growth of the filaments due to the polymerization which results in an advection of the distribution toward larger n with the frequency v. The two additional terms account for the severing: First, $b_n(t)$ is decreased because filaments of size n are cut at any of the nf_n occupied bonds with the characteristic frequency β; second, $b_n(t)$ increases when

any filament of size k, larger than n, whose $(n+1)^{\text{th}}$ bond (counted from the membrane) is occupied by a gelsolin molecule (which occurs with the probability f_k) is cut, at that specific position, after the time $1/\beta$.

The dynamics of the fraction f_n is more difficult to account for and, in order to make the result understandable, we shall detail the contributions of the various mechanisms. Consider the variation of the number, nf_nb_n, of gelsolin molecules attached to filaments having the size n. The addition of a monomer at the base does not change the number of gelsolin molecules so that the contribution of the polymerization is:

$$\left.\frac{d}{dt}(nf_nb_n)\right|_{pol.} = v(n-1)f_{n-1}b_{n-1} - vnf_nb_n. \tag{3}$$

The severing of a filament having the size n, at any of its occupied bonds, leads to the loss of the number nf_n of gelsolin molecules for the considered population, so that the first contribution of the severing is:

$$\left.\frac{d}{dt}(nf_nb_n)\right|_{sev.1} = -(\beta nf_n)nf_nb_n \tag{4}$$

where the prefactor (βnf_n) takes into account that the filament is likely to be cut at nf_n bonds with the characteristic time $1/\beta$. The severing of a filament having the size k, larger than n, at the $(n+1)^{\text{th}}$ bond, leads to a filament of size n whose bonds are occupied by a gelsolin molecule with the probability f_k, so that the second contribution of the severing is:

$$\left.\frac{d}{dt}(nf_nb_n)\right|_{sev.2} = \sum_{k=n+1}^{\infty}(\beta f_k)nf_kb_k \tag{5}$$

where the prefactor (βf_k) accounts for the fact that the $(n+1)^{\text{th}}$ bond is occupied with the probability f_k and cut with the characteristic time $1/\beta$ if so. Finally, the gelsolin molecules that are in solution, in the vicinity of the core, attach to the available bonds [number $n(1-f_n)$] with the characteristic time $k_{on}g_0$, where g_0 is the local concentration of the gelsolin, which leads to:

$$\left.\frac{d}{dt}(nf_nb_n)\right|_{att.} = (k_{on}g)n(1-f_n)b_n \tag{6}$$

Summing all the contributions listed in the Eqs. (3) to (6), we get the equation governing the dynamics of f_nb_n

$$\frac{d}{dt}(nf_nb_n) \;=\; v[(n-1)f_{n-1}b_{n-1} - nf_nb_n]$$

$$-\beta n^2 f_n^2 b_n + \beta n \sum_{k=n+1}^{\infty} f_k^2 b_k \qquad (7)$$
$$+k_{on} g_0 n(1-f_n) b_n.$$

The coupled equations (2) and (7) govern the dynamics of the distribution b_n and of the fraction f_n. We point out that Eqs. (2) and (7) couple the internal dynamics of the core with that of the diffusion fields in the cloud through the local concentration of the gelsolin g_0 and the velocity v which might depend on the local concentration of the actin monomer c_0.

3.2. The cloud

The dynamics of the cloud can be accounted for by considering, in addition to the severing, the diffusion of the various species in solution. Before we establish the boundary conditions, we first consider the concentration of the gelsolin, g, the concentration of the actin monomers and filaments, c_n, and then the fraction of occupied bonds, h_n.

The gelsolin molecules, on the one hand, diffuse with the diffusion coefficient D_g, detach from the bond when a filament is cut and attach to the available bonds of the filaments in solution. Thus, because of the severing process, the diffusing filaments constitute volume sources and sinks and the field $g(\vec{r},t)$ is governed by:

$$\frac{\partial g}{\partial t} = D_g \Delta g + \beta \sum_{k=1}^{\infty} h_k k c_k - k_{on} g \sum_{k=1}^{\infty} [1-h_k] k c_k \qquad (8)$$

where Δ denotes the Laplacian operator.

At the same time, the filaments diffuse in the cytoplasm, are cut with the characteristic time $1/\beta$ at any of the $nh_n(\vec{r},t)$ occupied bonds, so that:

$$\frac{\partial c_n}{\partial t} = \vec{\nabla}.[D_n \vec{\nabla} c_n] - \beta n h_n c_n + 2\beta \sum_{k=n+1}^{\infty} h_k c_k. \qquad (9)$$

Note that the diffusion coefficient depends on space. Indeed, D_n depends on the fraction of bonds occupied by the gelsolin (Eq. 1). The factor 2 in the last term is due to the fact that there are two possibilities for getting a filament of size n when cutting a larger filament. Finally, we mention that the equation (9) holds true for the monomer and that we get for $n = 0$:

$$\frac{\partial c_0}{\partial t} = D_0 \Delta c_0 + 2\beta \sum_{k=1}^{\infty} h_k c_k. \qquad (10)$$

The dynamics of the fraction h_n is again more difficult to account for and we shall detail the contributions of the various mechanisms. We consider the contributions of all the mechanisms that induce a variation of the number nh_nc_n, in the unit volume, of gelsolin molecules attached to the filaments of size n. The filaments diffuse and carry, each, a number $nh_n(\vec{r},t)$ molecules:

$$\frac{\partial}{\partial t}(nh_nc_n)\Big|_{diff.} = \vec{\nabla}.(nh_nD_n\vec{\nabla}c_n) \tag{11}$$

Again, the diffusion does not reduce to a simple Laplacian equation, not only because the diffusion coefficient depends on space and time but also because the number of gelsolin molecules on the filaments depends on space and time. In addition, the severing of the filaments having the length n leads, on the one hand, to the decrease of the local concentration of the gelsolin attached to the filaments of size n according to:

$$\frac{\partial}{\partial t}(nh_nc_n)\Big|_{sev.1} = -\beta n^2h_n^2c_n. \tag{12}$$

Indeed, $nh_n(\vec{r},t)$ gelsolin molecules are attached to the filament which is thus cut with the frequency $\beta nh_n(\vec{r},t)$, $nh_n(\vec{r},t)$ gelsolin molecules being transfered to smaller filaments or released in solution. On the other hand, the severing of larger filaments ($k > n$), at two specific positions occupied with the probability $h_k(\vec{r},t)$, leads to a filament of size n and provides $nh_k(\vec{r},t)$ gelsolin molecules:

$$\frac{\partial}{\partial t}(nh_nc_n)\Big|_{sev.2} = \sum_{k=n+1}^{\infty} \beta(nh_k)(2h_k)c_k \tag{13}$$

Finally, free gelsolin molecules attach to the filaments at the available bonds:

$$\frac{\partial}{\partial t}(nh_nc_n)\Big|_{att.} = k_{on}gn(1-h_n)c_n \tag{14}$$

From the contributions Eqs. (11) to (14), we get the equation governing the product h_nc_n:

$$\begin{aligned}\frac{\partial}{\partial t}(nh_nc_n) &= \vec{\nabla}.[nh_nD_n\vec{\nabla}c_n] - \beta n^2h_n^2c_n \\ &\quad +2\beta n\sum_{k=n+1}^{\infty} h_k^2c_k + k_{on}gn[1-h_n]c_n\end{aligned} \tag{15}$$

The equations (2) and (7) govern the dynamics of the distribution $b_n(t)$ and of the fraction $f_n(t)$ in the core whereas the equations (8), (9) and (15) govern the dynamics of $c_n(\vec{r},t)$ and $g(\vec{r},t)$, the actin and gelsolin concentration fields, and the fraction $h_n(\vec{r},t)$ in the cloud.

3.3. The boundary conditions

Due to the polymerization, the core acts as a sink of monomeric actin whereas, due to the severing, it acts as a source of both actin monomers and filaments. In the same way, due to the attachment to the available bonds, the core acts as a sink of gelsolin molecules but, due to the severing process, is a source of gelsolin, free or attached to diffusing filaments. In order to account for these sources and sinks, we shall write the boundary conditions at the core, supposed to be centered in $\vec{r} = \vec{0}$.

Diffusing filaments are released in solution when filaments of the core are cut at the appropriate bond whereas, the total number of filaments in the core being M and v monomers being added per unit time, Mv monomers are consumed:

$$\int_S D_n(\vec{\nabla} c_n).d\vec{S} = Mv\,\delta(n) - M\beta \sum_{k=n+1}^{\infty} f_k b_k \tag{16}$$

where S is a surface enclosing the core and, $d\vec{S}$ the surface element oriented outwards. The diffusion coefficient, which depends on $h_n(\vec{r},t)$, is evaluated at the boundary. The first term on the right-hand side accounts for the consumption of monomers (δ stands for the Kronecker delta function) due to the polymerization.

The severing of a longer filament ($k > n$) in the core, after a time $1/\beta$ if the bond is occupied (which occurs with the probability f_k) releases in solution nf_k gelsolin molecules which then diffuse attached to the filament:

$$\int_S n h_n D_n(\vec{\nabla} c_n).d\vec{S} = -nM\beta \sum_{k=n+1}^{\infty} f_k^2 b_k. \tag{17}$$

Finally, per unit time, $k_{on} g_0$ gelsolin molecules attach to any available bond in the core [$g_0 \equiv g(0,t)$ stands for the gelsolin concentration at the core] whereas one molecule is released in solution each time a bond is cut:

$$D_g \int_S \vec{\nabla} g.d\vec{S} \;=\; -M\beta \sum_{n=1}^{\infty} n f_n^2 b_n \tag{18}$$

$$+Mk_{on}g_0\sum_{n=1}^{\infty} n(1-f_n)b_n$$

Far away from the core, the concentration of any filament vanishes, whereas the concentrations of the monomers and of the gelsolin tend respectively to the overall concentrations c_0^∞ and g^∞:

$$\lim_{r\to\infty} c_n(\vec{r},t) = c_0^\infty \delta(n) \tag{19}$$

$$\lim_{r\to\infty} g(\vec{r},t) = g^\infty \tag{20}$$

We mention also that, accordingly, the concentration of gelsolin molecules attached to filaments of size n also vanishes so that $\lim_{r\to\infty}(nh_nc_n) = 0$ $(\forall n)$.

4. Parameters of the problem

From now on, it is particularly interesting to consider the parameters of the problem. First, the equation governing the internal dynamics of the core [Eqs. (2) and (7)] suggest that the pertinent timescale is $\tau = 1/\beta$ whereas the equation governing the actin diffusion field [Eqs. (9) and (15)] suggest that the pertinent length-scale is $\sqrt{D_0/\beta}$. We shall thus report results expressed in terms of the dimensionless variables $\tilde{t} \equiv \beta t$ and $\tilde{r} \equiv r\sqrt{\beta/D_0}$. Second, one can consider that the pertinent concentration scale is the concentration of the actin far away from the core so that one can express all the concentrations relative to c_0^∞. We thus define, for instance, $\tilde{c}_n = c_n/c_0^\infty$ and $\tilde{g} = g/c_0^\infty$.

The remaining independent parameters of the problem are α, D_g, g^∞, M, σ, k_{on} and the function v. The parameter α is the ratio of the gelsolin and actin molecular weights which plays a role in the dependency of D_n on h_n. We define $d \equiv D_g/D_0$, $\gamma \equiv g^\infty/c_0^\infty$ and $\zeta \equiv k_{on}g^\infty/\beta$ in accordance with the choice of the dimensionless variables. The parameters M and σ account for the surface density of the actin filaments inside the podosome core. Indeed, assuming that $\sigma \ll \sqrt{D_0/\beta}$ one can consider that the surface in the boundary conditions [Eqs. (16) to (18)] is a sphere of radius $\sigma/2$. Assuming then radial diffusion fields, one exhibits the dimensionless parameter $\Phi \equiv (2M/\pi\sigma^2)/(\sqrt{D_0/\beta}\, c_0^\infty)$ which compares the density of the filaments in the core with the surface density of the actin monomer in a layer of thickness $\sqrt{D_0/\beta}$.

5. Results

We shall first study the steady-state solution to the problem and then discuss the characteristic time associated with the dynamics of the system. The solutions of the problem are calculated numerically.

5.1. The core

The internal dynamics of the core, governed by the equations (2) and (7), is coupled to the cloud only by the velocity v which might depend on the local concentration of the actin monomer and by the local concentration of the gelsolin, g_0. Thus, it is pertinent to consider the steady-state solution for given $v^* \equiv v/\beta$ and $\zeta_0 \equiv k_{on} g_0/\beta$. In the figure 3a, we report typical solutions for b_n and $f_n b_n$ as functions of n in the steady state. We observe that the distribution b_n presents the same typical shape already described in [10]. From the similarity of the shapes of b_n and $f_n b_n$, we can conclude that f_n does not drastically depend on n and, thus, that the gelsolin bound to the filaments is rather homogeneously distributed among the filaments having different lengths. We define and report the podosome size, $\overline{n} \equiv \sum_{n=0}^{\infty}(n+1)b_n$, and the average fraction of gelsolin on the filaments in the core, $f_g \equiv (\sum_{n=0}^{\infty} n f_n b_n)/(\sum_{n=0}^{\infty} n b_n)$ (Fig. 3b). We find numerically that f_g and $\overline{n}/\sqrt{\pi v^*/2}$ are functions of $\zeta_0/\sqrt{v^*}$ which can be understood as the product of the attachment characteristic frequency $k_{on} g_0$ and of the characteristic time of the core growth $\tau_{core} \equiv 1/\sqrt{\beta v}$ ($\propto \overline{n}/v^*$). For $\zeta_0/\sqrt{v^*} \gg 1$, the gelsolin tends to occupy all the bonds so that $f_g \simeq 1$ and $\overline{n} \simeq \sqrt{\pi v^*/2}$ as we already demonstrated analytically [10]. For smaller $\zeta_0/\sqrt{v^*}$, the concentration $f_g < 1$, which leads to a less effective severing process and, accordingly, to a larger typical core size $\overline{n}$.

Thus, the characteristics of the podosome core do not depend drastically on the local concentration of the gelsolin, g_0. Indeed, changing ζ_0 by a factor 10^4 (from 100 to 0.01) changes $\overline{n}$ by a factor 5 only. By contrast, $\overline{n} \propto v^{*1/2}$ and, thus, the characteristic time of the podosome growth, $\tilde{\tau}_{core} \sim v^{*-1/2}$ drastically depend on the polymerization velocity which might depend on the local concentration of the actin monomer.

5.2. The cloud

The dynamics of the actin and of the gelsolin in the surrounding core is governed by the equations (8), (9) and (15). The podosome core, assumed to be centered in $\vec{r} = \vec{0}$, is accounted for by the boundary conditions (16) to (20).

Considering again the steady state, we can report the typical concentration c_n of the actin filaments of size n and the concentration nh_nc_n of gelsolin bound to the filaments of size n in the cloud as functions of the distance to the core $\tilde{r}$. In the figure 4a, one observes that the diffusion length associated with the longer filaments (larger n) is shorter. This can be understood easily considering the fact that the gelsolin can cut the longer filaments in a larger number of locations. Thus, the longer filaments have a smaller probability to reach a large distance from the core. By contrast to c_n, each concentration nh_nc_n has a non-monotonic dependency on the distance $\tilde{r}$ and reaches a maximum at a finite distance from the core (Fig. 4b). The increase near the core is due to the continuous binding of free gelsolin molecules whereas, far from the core, the decrease results from the decrease of the filament concentration c_n. We define and report the total concentration of the actin monomer, $c_a \equiv \sum_{n=0}^{\infty}(n+1)c_n$, and of the gelsolin, $c_g \equiv g + \sum_{n=0}^{\infty} nh_nc_n$, as functions of the distance r from the podosome core (Fig. 4c). We note that both the actin and the gelsolin accumulate around the core in a region having a dimensionless radius, denoted $\tilde{r}_c$, which is governed by the competition between the diffusion and the severing: The typical diffusion-coefficient is of the order of $D_0/\overline{n}$ whereas the typical severing frequency is about $\overline{n}\beta$. Considering that r_c is of the order of the associated diffusion lengh $\sqrt{D_0/\beta}/\overline{n}$, we get $r_c \sim \sqrt{D_0/v}$ and, thus, $\tilde{r}_c \sim 1/\sqrt{v^*}$. Interestingly, considering the dynamics, one can estimate the time necessary to establish the steady-state diffusion field to be of the order of $\tau_{cloud} \sim r_c^2/(D_0/\overline{n})$ so that $\tilde{\tau}_{cloud} \sim \tilde{\tau}_{core}$. Thus, provided that the polymerization frequency v is given, the dynamics of the whole system involves a single characteristic time $\tau = 1/\sqrt{\beta v}$. We point out that, the typical number $\overline{n}$ being a slowly varying function of the gelsolin concentration at the core, the typical size and, thus, the characteristic time associated with the cloud dynamics depend only slowly on the local concentration of the gelsolin.

6. Discussion

In a former publication [10], two of us and a co-worker presented the only-available model of the turnover of the actin within the podosomal structure. They showed that such models can explain, for instance, that the typical height of the core is auto-regulated by the interplay between the polymerization and severing processes or why the steady-state core might have a finite lifespan. However, the model was too simplistic to account for the collocal-

ization of the actin and gelsolin molecules or to envisage a modeling of the podosomes collective-dynamics in a so simple framework.

Here, we presented a model of the podosome dynamics including not only the actin turnover but also the gelsolin dynamics. We show that the polymerization of actin filaments at the cell membrane and the diffusion and attachment kinetics of the gelsolin account for the observation of large concentrations of the actin and of the gelsolin in the podosome region, in both the core and the cloud. The model is thus compatible with the collocalization of the molecules observed in the fluorescence microscope. In addition, the model predicts that the characteristics of the podosome in the steady-state, typical size and characteristic time for instance, are not sensitive to the local concentration of the gelsolin. The main conclusions of the former publication still hold true when the dynamics of the gelsolin is taken into account. The present model might easily be modified in order to include the capping.

The interplay between the gelsolin and actin concentration fields is now accounted for. We then think that the present model includes the ingredients that make it possible to envisage a modeling of the podosomes collective-dynamics based on a system of equations similar to that presented here. The dependency of the polymerization frequency on the local concentration of actin at the core and the interaction between cores through the diffusion fields in the cloud might explain the collective dynamics of the system. Especially, the formation and the migration of podosome rings [5] in the framework of the present model shall be investigated in the near future.

Acknowledgments

J.-C.G. and X.W. acknowledge the support from the CNRS and the NSFC (contract #020041FSD). S.H. aknowledges support from the "Région Rhône-Alpes" (Programme MIRA).

References

[1] Marchisio, P.C., Cirillo, D., Naldini, L., Primavera, M.V., Teti, A. and Zambonin-Zallone, A., J. Biol. Phys. **99** (1984) 1696-1705.

[2] Marchisio, P.C., Cirillo, D., Teti, A., Zambonin-Zallone, A. and Tarone, G., Exp. Cell Res. **169**(1987) 202-214.

[3] Nermut,M.V., Eason, P., Hirst, E.M. and Kellie, S., Exp. Cell Res. **193** (1991) 382-397.

[4] Tarone, G., Cirillo, D., Giancotti, F.G., Comoglio, P.M. and Marchisio, P.C., Exp. Cell Res. **159** (1985) 141-157.

[5] Destaing O., Saltel F., Géminard J.-C., Jurdic P. and Bard F., Mol. Biol. Cell**14** (2003) 407-416.

[6] Pfaff, M. and Jurdic, P., J. Cell Sci. **114**(2001) 2775-2786.

[7] Luxenburg, C., Geblinger D., Klein E., Anderson K., Hanein D., Geiger B. and Addadi L., PLoS ONE **2** (2007) e179.

[8] Chellaiah, M., Kizer, N., Silva, M., Alvarez, U., Kwiatkowski, D. and Hruska, K.A., J. Cell Biol. **148** (2000) 665-678.

[9] Gavazzi, I., Nermut, M.V. and Marchisio, P.C., J. Cell Sci. **94** (1989) 85-89.

[10] Biben T., Géminard J.-C. and Melo F., J. Biol. Phys. **31** (2005) 87-120.

[11] E. Urban *et al*, Nat. Cell Biol., **12** (2010) 429-435.

[12] *Molecular Biology of the Cell, 3rd Ed.*, Editors: Alberts B., Bray D., Lewis L., Raff M., Roberts K. and Watson J.D., Garland Publishing (New-York, 1994), p.845.

[13] S. Ono, Int. Rev. Cytol. **258** (2007) 1-82.

[14] Einstein A., Ann. Phys. **17** (1905) 549.

Figure captions

Figure 1: Fluorescence images of an osteoclast - The podosomes correspond to the bright dots. The use of two dyes exhibiting different fluorescence wavelengths makes it possible to image separately the actin (A) and the gelsolin (G). The experiment clearly demonstrates the colocalization of the actin and gelsolin fluorescence signals in the podosome core [Fixed osteoclast observed in an *Axioplan 2 Imaging* from *Zeiss*: actin marked with Phalloidin (wavelength 488 nm) and gelsolin with Anti-Gelsolin bound with fluorescent second antibody (wavelength 562 nm)]

Figure 2: Sketch of the podosomal structure.

Figure 3: Typical solution for the podosome core - (a) Typical b_n and $f_n b_n$ ($v^* = 1000$, $\zeta_0 = 10$). (b) Fraction f_g (open squares) and normalized size $\overline{n}/\sqrt{\pi v^*/2}$ (full diamonds) vs. $\zeta_0/\sqrt{v^*}$.

Figure 4: Typical solution for the cloud - (a) Concentration of the actin filaments $\tilde{c}_n$ in the cloud. (b) Concentration $nh_n\tilde{c}_n$ of gelsolin bound to the filaments of size n in the cloud. (c) Total concentrations of the gelsolin $\tilde{c}_g$ and of the actin $\tilde{c}_a$ in the cloud around the core. One can notice that, in spite of the small concentration of gelsolin far away from the podosome ($\gamma = 5.855\ 10^{-2}$), the concentrations of the actin and of the gelsolin in the core region are of the same order ($v^* = 1000$, $\zeta_0 = 10$, $\alpha = 0$, $d = 1$, $\phi = 2.516\ 10^{-3}$, $\zeta = 1.171\ 10^2$ and $\gamma = 5.855\ 10^{-2}$. These parameters insure $\zeta_0 = 10$ which corresponds to the core described in Fig. 3).

Figure 1

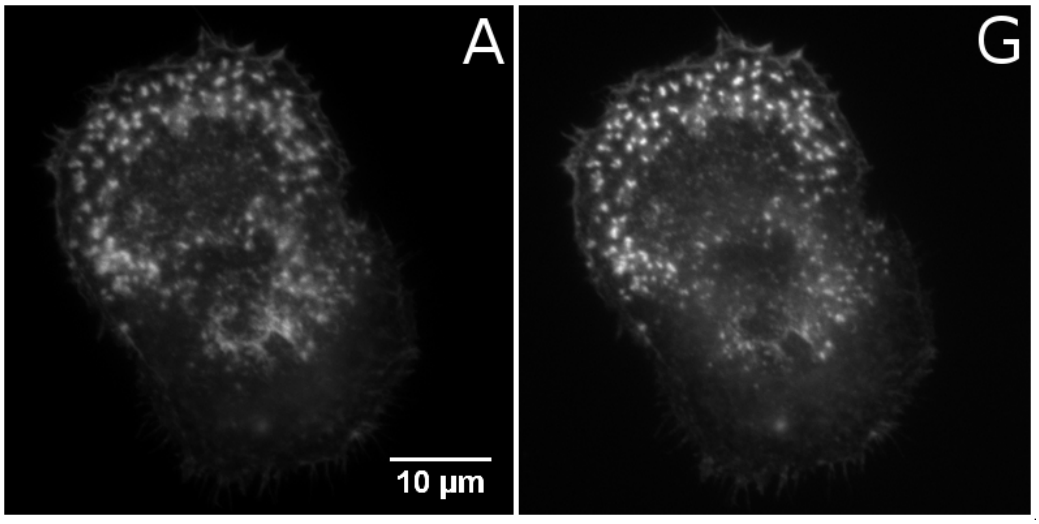

Figure 2

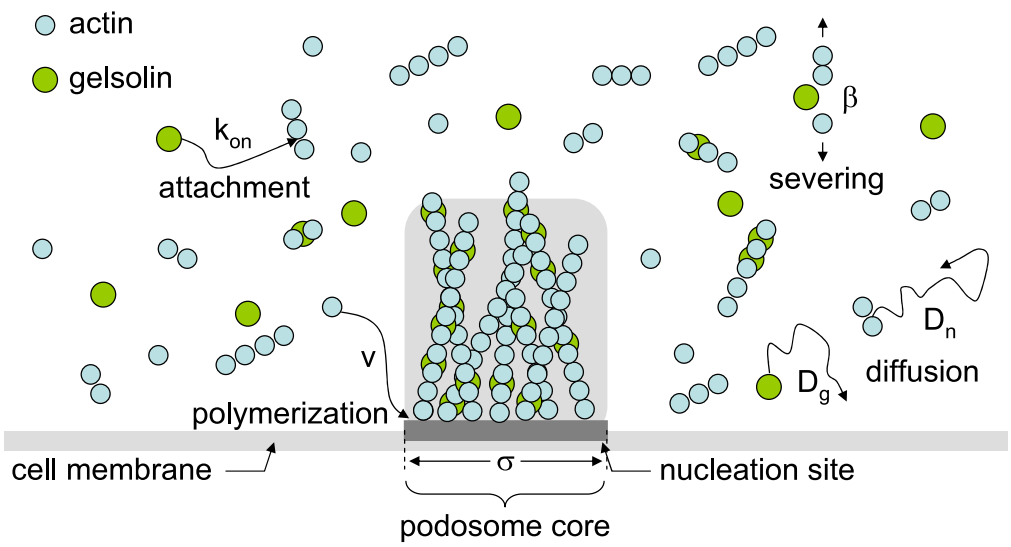
actin
gelsolin
k_{on}
attachment
β
severing
D_n
diffusion
D_g
v
polymerization
cell membrane
σ
nucleation site
podosome core

Figure 3

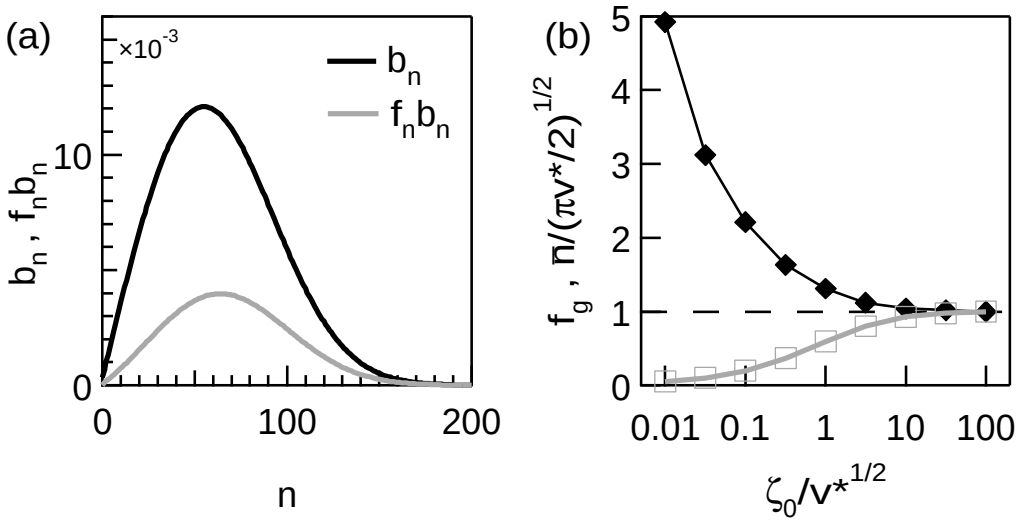
(a)
×10^-3
b_n
f_n b_n
b_n , f_n b_n
10
0
0
100
200
n
(b)
5
4
3
2
1
0
f_g , π/(πν*/2)^1/2
0.01
0.1
1
10
100
ζ_0/ν*^1/2

Figure 4

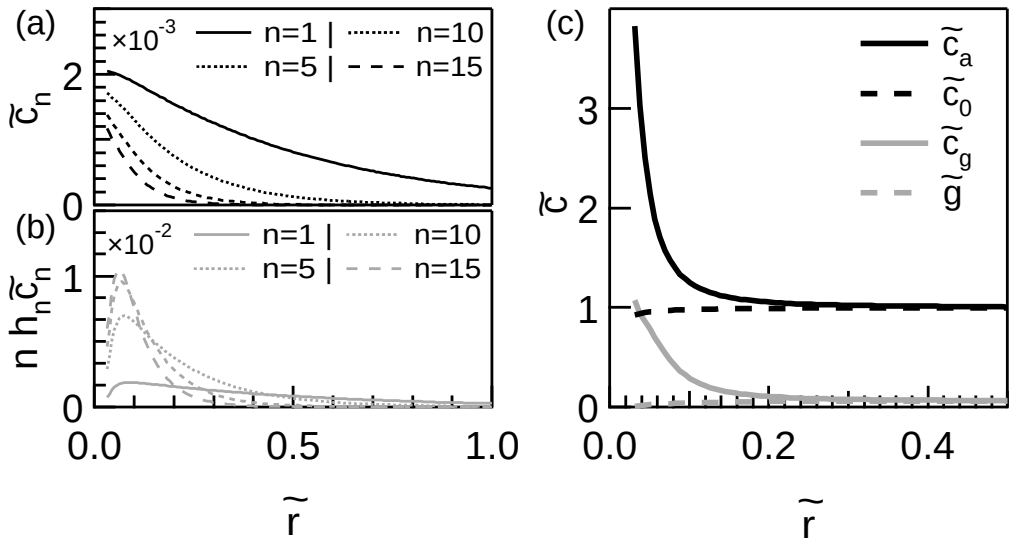
(a)
×10^-3
n=1 | n=10
n=5 | n=15
c̃n
2
0
(b)
×10^-2
n=1 | n=10
n=5 | n=15
n h̃n c̃n
1
0
0.0
0.5
1.0
r̃
(c)
c̃a
c̃0
c̃g
g̃
c̃
3
2
1
0
0.0
0.2
0.4
r̃